Supporting Information

Fernández-Busnadiego et al. 10.1073/pnas.1503191112

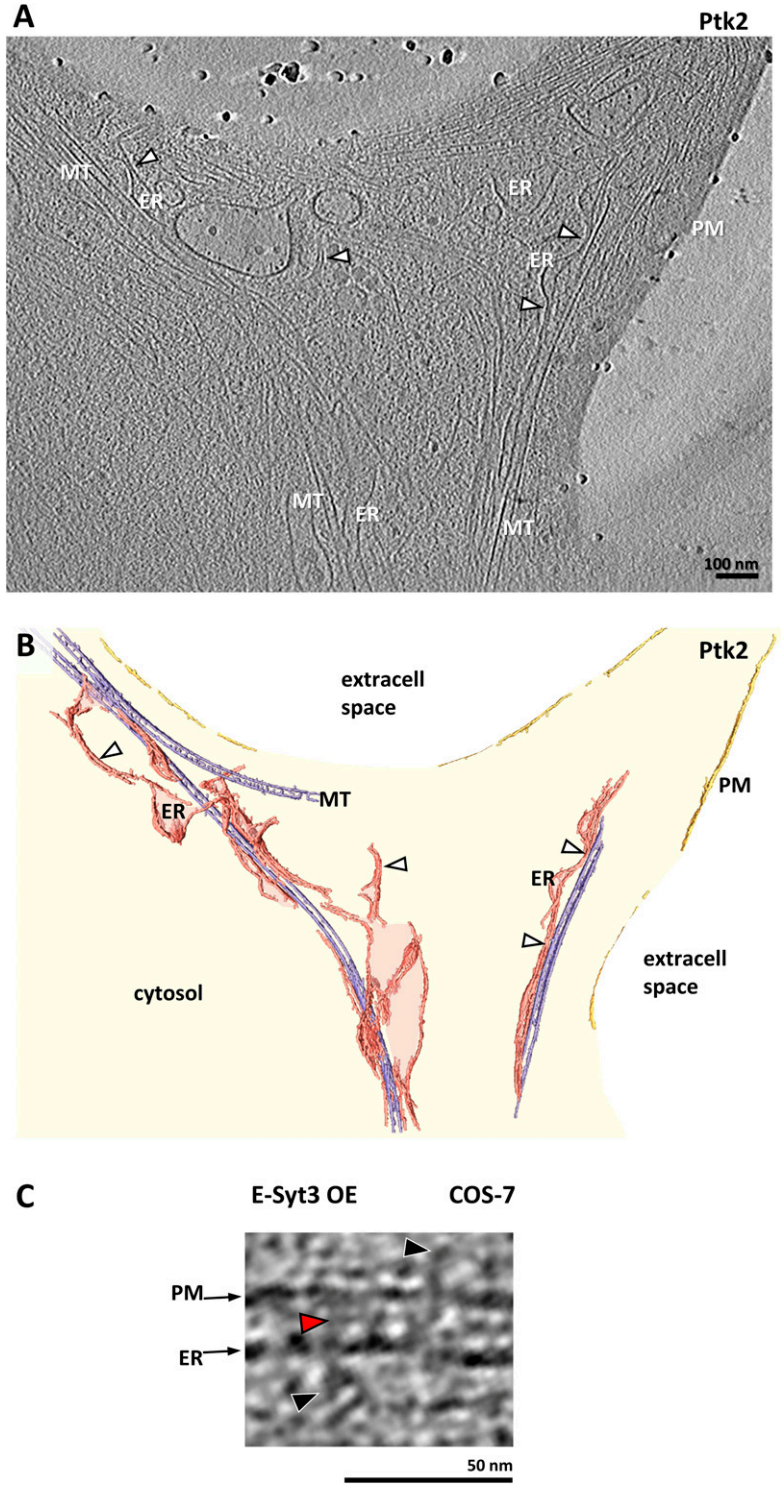

Fig. S1. ER morphology at the cell edge in an untransfected Ptk2 cell and detail of a contact in a COS-7 cell overexpressing E-Syt3. (*A*) Tomographic slice (2.4 nm thick) of the edge of an untransfected Ptk2 cell. (*B*) 3D rendering of the tomogram shown in *A*. Narrow ER tubules are indicated by white arrowheads. (*C*) Higher-resolution tomographic slice (2.1 nm thick) from data recorded with a direct electron detector on a COS-7 cell transfected with Myc-E-Syt3 (E-Syt3 OE). The intermediate density is indicated by a red arrowhead, and the extracellular or ER luminal densities apparently connected to bridges of the intermediate density to the ER and PM are indicated by black arrowheads.

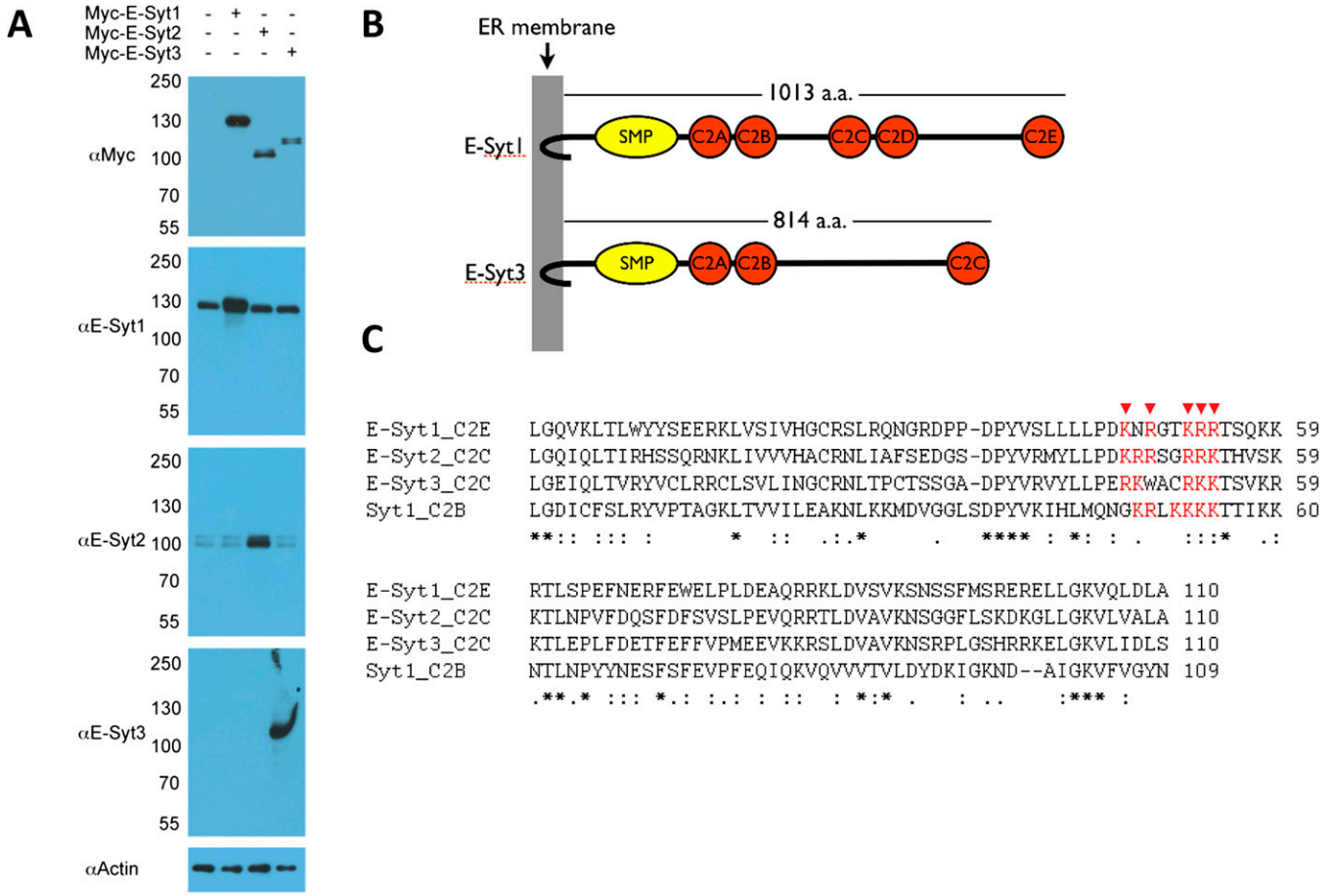

Fig. S2. E-Syt overexpression in COS-7 cells and E-Syt domain structure. (*A*) Lysates of COS-7 cells transfected with the indicated constructs were processed for SDS/PAGE and immunoblotted with anti-Myc (αMyc), anti–E-Syt1 (αE-Syt1), anti–E-Syt2 (αE-Syt2), or anti–E-Syt3 (αE-Syt3) antibodies and with anti-actin (αActin) as a loading control. Bands with the expected molecular weight were detected (i.e., native E-Syt1: 121 kDa; native E-Syt2 and E-Syt3: 100 kDa). (*B*) Structure of the E-Syt1 and E-Syt3 domains. The numbers indicate the predicted length of their cytosolic portion in amino acids. (*C*) Sequence alignment of the C2E domain of E-Syt1, the C2C domains of E-Syt2/3, and the C2B domain of Syt1 by ClustalW2. The cluster of basic residues (red) at the basic patch of the E-Syt1 C2E domain is indicated by red arrowheads. Asterisks, colons, and periods denote residues that are identical, strongly similar, or weakly similar, respectively, based on the PAM 250 matrix.

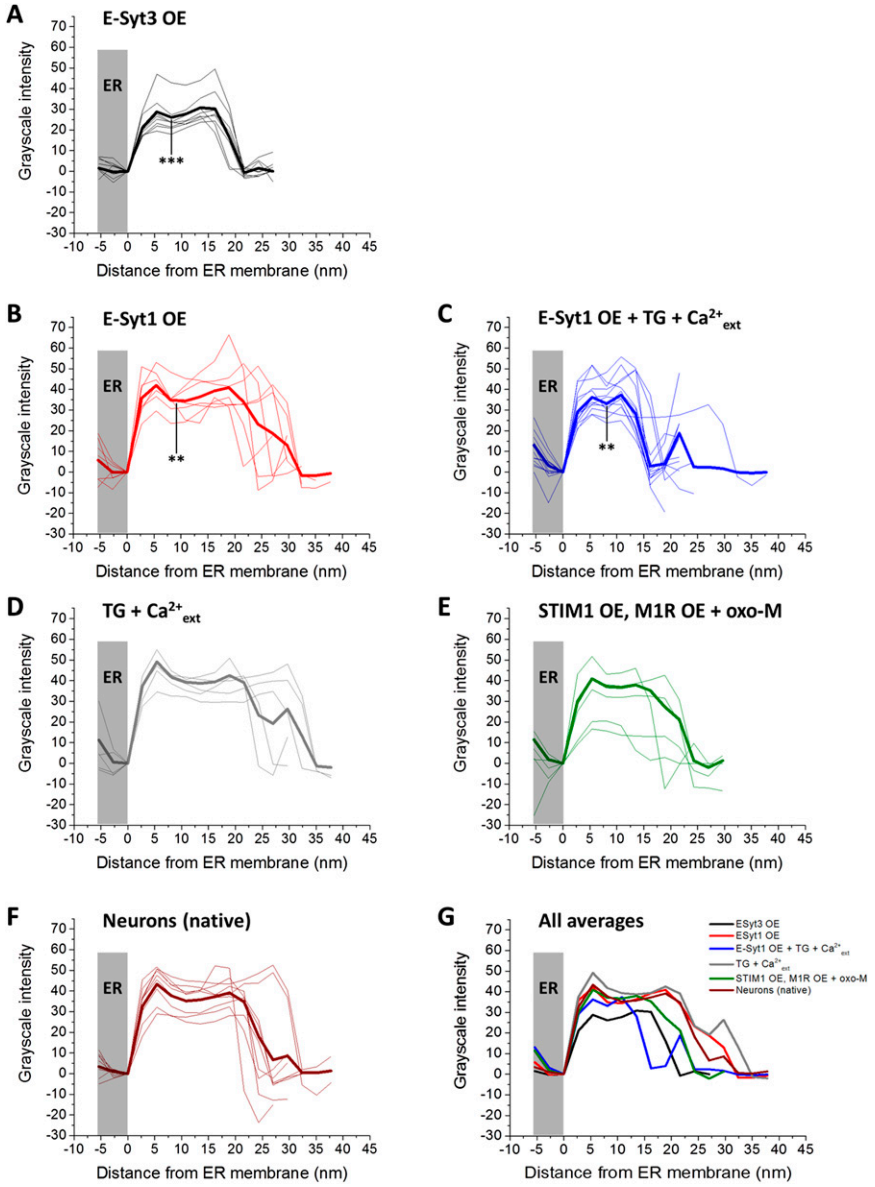

Fig. S3. Grayscale intensity profile of ER–PM contacts, normalized to the intensity of the ER membrane. Low grayscale intensity corresponds to darker, more electron-dense regions (e.g., membranes) in the tomograms. In *A–F*, thin lines represent individual tomograms, and thick lines represent their averages. A shaded area represents the ER membrane (first global minimum of the curves), with grayscale intensity normalized to 0. Grayscale intensity is similarly low at the PM (second global minimum) and higher in the cytosol (region flanked by the two global minima). Conditions are as follows: (*A*) Myc-E-Syt3 overexpression (E-Syt3 OE; $n = 8$); (*B*) Myc-E-Syt1 overexpression (E-Syt1 OE; $n = 7$); (*C*) Myc-E-Syt1 overexpression and elevation of cytosolic Ca^{2+} by a TG-based protocol (E-Syt1 OE + TG +Ca^{2+}_{ext}; $n = 13$); (*D*) no protein overexpression and elevation of cytosolic Ca^{2+} by a TG-based protocol (TG +Ca^{2+}_{ext}; $n = 5$); (*E*) mRFP-STIM1 and M1R overexpression and stimulation with Oxo-M (STIM1 OE, M1R OR + oxo-M, $n = 5$); (*F*) untransfected and untreated DIV13 mouse cultured neurons [Neurons (native), $n = 10$]. The average profiles for *A–F* are overlaid in *G*. Note that a layer significantly darker than the surrounding cytosol (intermediate density) was present only in the samples transfected with E-Syts. $^{**}P < 0.01$ and $^{***}P < 0.001$ by paired Student's *t* test.

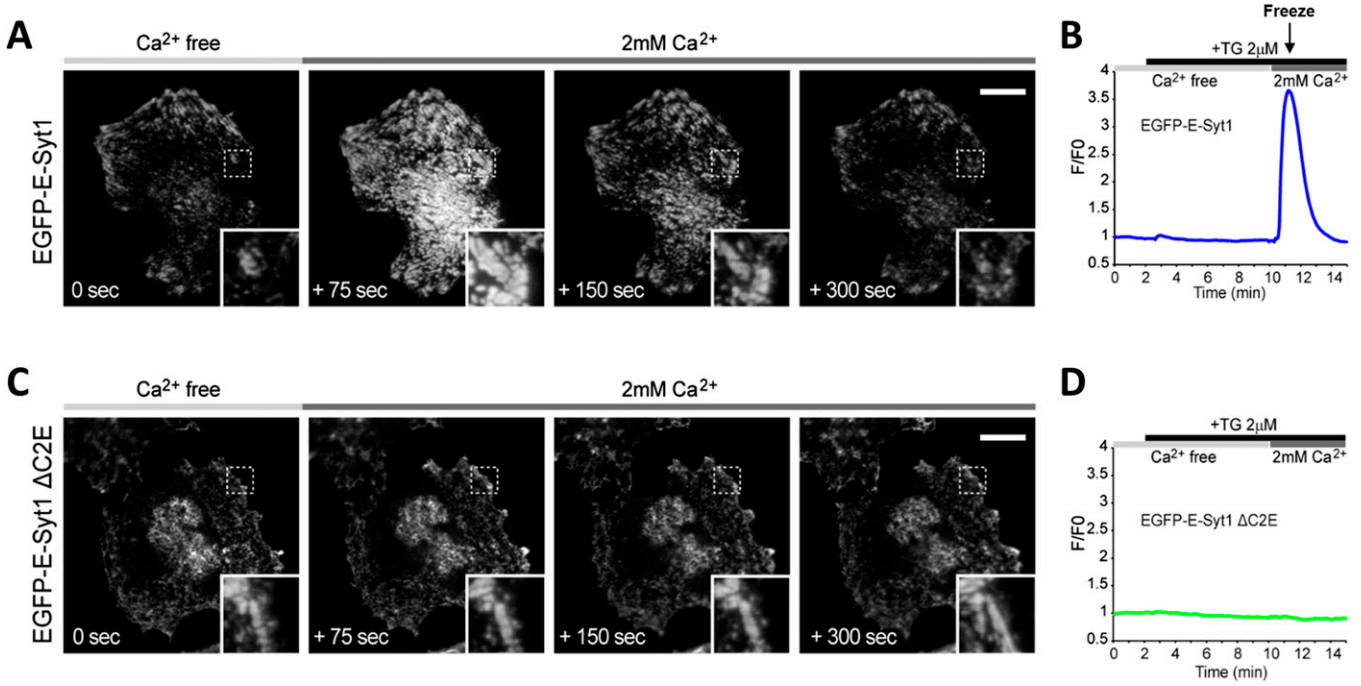

Fig. S4. Formation of E-Syt1–mediated ER–PM contacts by live-cell TIRF imaging. (*A*) TIRF microscopy images of a COS-7 cell expressing EGFP-E-Syt1 before and after readdition of 2 mM Ca^{2+} during treatment with 2 μM TG. (*B*) Time course of the recruitment of EGFP-E-Syt1 to the PM, as shown in *A*. (*C*) TIRF microscopy images of a COS-7 cell expressing EGFP-E-Syt1 with C2E domain deletion (EGFP-E-Syt1 ΔC2E) before and after readdition of 2 mM Ca^{2+} during treatment with 2 μM TG. (*D*) Time course of the recruitment of EGFP-E-Syt1 ΔC2E to the PM, as shown in *C*. Note that deletion of the C2E domain led to the loss of the recruitment of EGFP-E-Syt1 to the PM. The time point in which cells were frozen for cryo-ET in a parallel experiment is indicated in *B*. (Scale bars: 10 μm.)

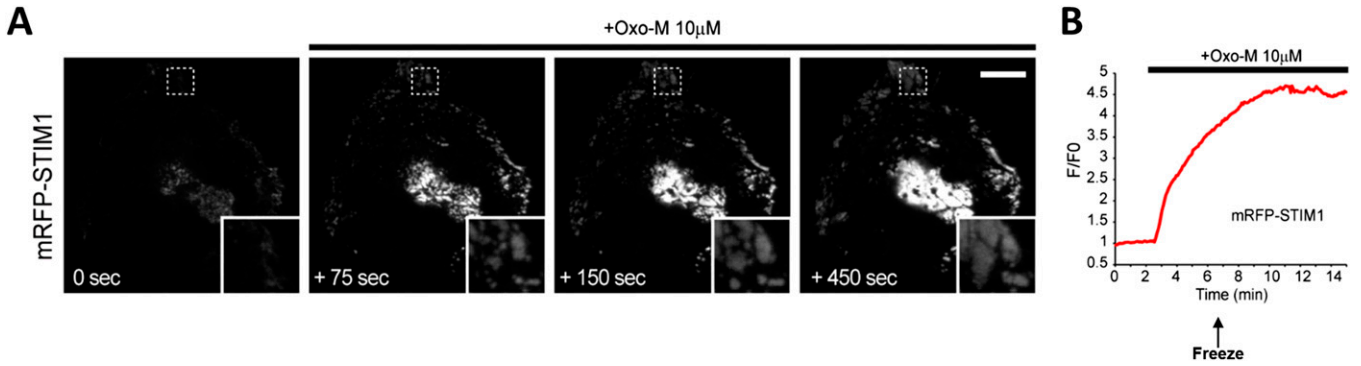

Fig. S5. Formation of STIM1-mediated ER–PM contacts by live-cell TIRF imaging. (*A*) TIRF microscopy images of a COS-7 cell expressing mRFP-STIM1 together with M1R before and after stimulation with 10 μM Oxo-M. (*B*) Time course of the recruitment of mRFP-STIM1 to the PM, as shown in *A*. The time point in which cells were frozen for cryo-ET in a parallel experiment is indicated in *B*. (Scale bar: 10 μm.)

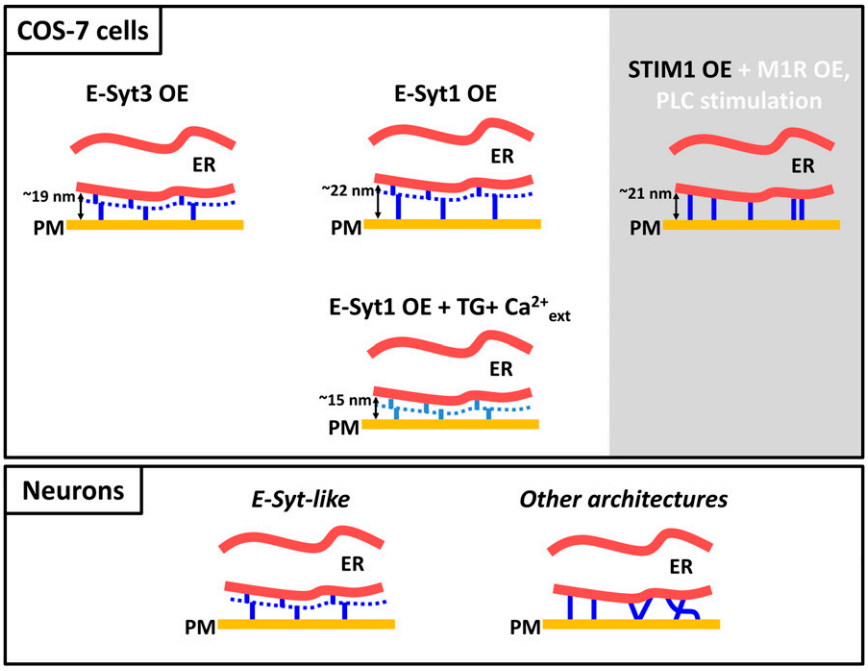

Fig. S6. Graphical summary. (*Upper*) Overexpression of ER–PM tethers in COS-7 cells. (*Upper Left*) In ER–PM contacts at cells overexpressing E-Syt3 (E-Syt3 OE), the average distance between the ER membrane (pink lines) and the PM (yellow line) was ∼19 nm. An electron-dense layer (blue dotted line) was observed at the contacts ∼8 nm away from the ER membrane. Filamentous bridges (blue solid lines) linked that intermediate density to the ER and the PM. ER–PM contacts in cells overexpressing E-Syt1 at resting Ca^{2+} levels (E-Syt1 OE) were structurally similar to those mediated by E-Syt3, but ER–PM distance was wider (∼22 nm), in agreement with the longer amino acid length of the cytosolic portion of E-Syt1. Triggering SOCE by TG (E-Syt1 OE + TG +Ca^{2+}_{ext}) resulted in a pronounced narrowing of the ER–PM distance (to ∼15 nm) and a weakening of the intermediate density (light blue). The difference in the distance between the intermediate density and the ER membrane in all E-Syts–mediated contacts was not statistically significant. (*Upper Right*) This intermediate density was not evident in STIM1-mediated contacts (STIM1 OE, M1R OR + PLC stimulation; PLC stands for phospholipase C). Instead, these contacts showed filaments (blue solid lines) linking the ER and the PM. In this condition, the ER–PM distance was ∼21 nm. (*Lower*) Untransfected DIV13 neurons (*Lower Left*) In untransfected neurons some contacts (E-Syt–like) showed an intermediate density between ER and the PM, similar to contacts found upon E-Syt overexpression in COS-7 cells. (*Lower Right*) Other contacts (Other architectures) showed filaments linking the membranes as in STIM1-mediated contacts in COS-7 cells and/or tethers of unidentified nature. Contacts in which different tethering architectures coexisted were also found in neurons. These findings indicate that the ER–PM contact architectures found upon overexpression are representative of some native contacts in untransfected cells.

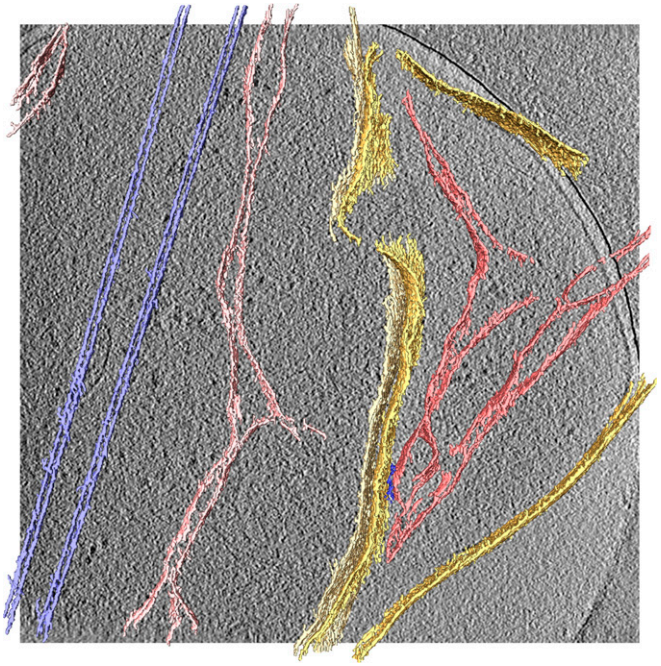

Movie S1. ER–PM contact in an untransfected COS-7 cell. The movie displays 2.7-nm-thick tomographic slices and a 3D rendering of the data shown in Fig. 1 *F* and *G*. The rendering displays PM (gold), ER (pink), and microtubules (light blue). Note the electron densities present at the ER–PM contact (displayed up to an arbitrary grayscale intensity threshold, dark blue). The complete field of view is 1.8 μm.

Movie S1

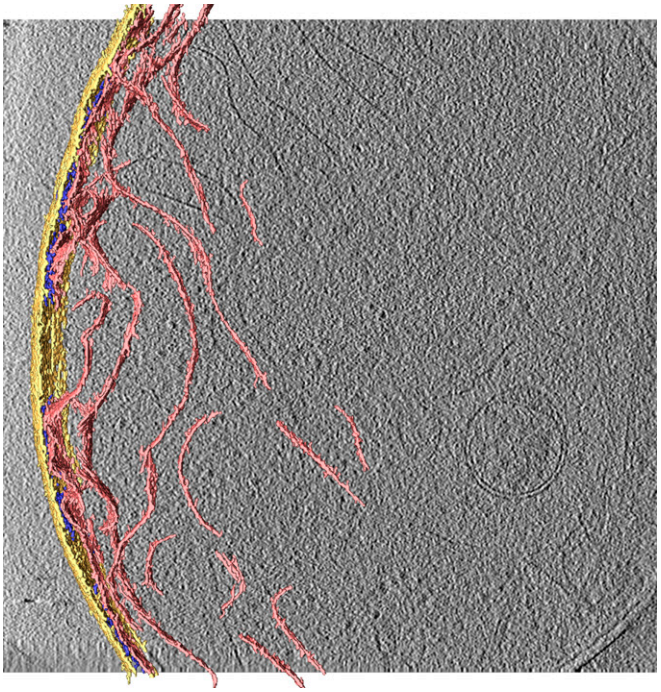

Movie S2. ER–PM contact in an Myc-E-Syt3–transfected COS-7 cell. The movie displays 2.7-nm-thick tomographic slices and a 3D rendering of the data shown in Fig. 2 *A* and *B*. Note the large size of the ER–PM contact in comparison with those found in untransfected COS-7 cells. The complete field of view is 1.8 μm.

Movie S2

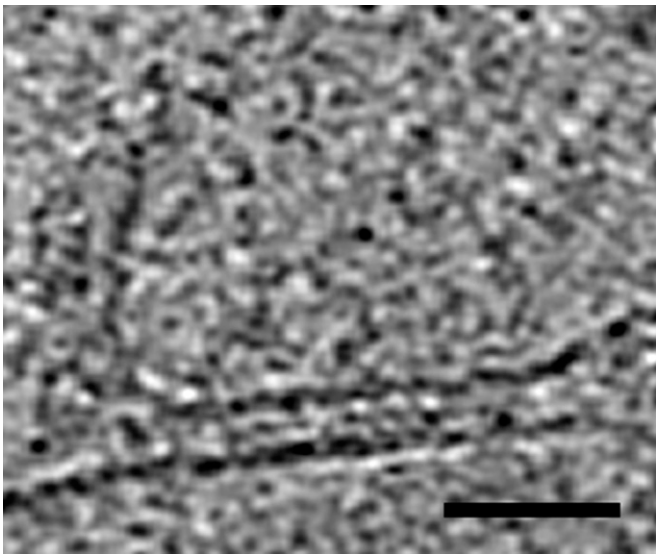

Movie S3. Detail of an ER–PM contact in an Myc-E-Syt3–transfected COS-7 cell. The movie displays 2.1-nm-thick tomographic slices shown in Fig. 2 *C* and *D* (recorded with a direct electron detector). As in Fig. 2*C*, the PM is at the bottom, and the ER is above. Note the intermediate density between the ER and the PM and the filamentous bridges connecting it to both membranes. (Scale bar: 50 nm.)

Movie S3

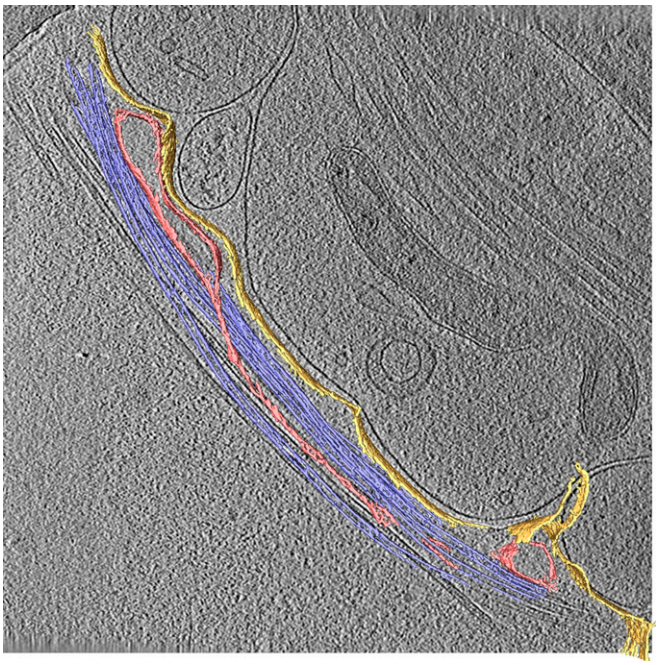

Movie S4. ER–PM contact in an untransfected cultured neuron. The movie displays 2.7-nm-thick tomographic slices and a 3D rendering of the data shown in Fig. 5 *A* and *B*. Note the intermediate density between the ER and the PM, reminiscent of that found in E-Syt–transfected COS-7 cells. The complete field of view is 1.8 μm.

Movie S4